16TH EUROPEAN CONFERENCE ON EARTHQUAKE ENGINEERING THESSALONIKI 18 - 21 JUNE 2018

ANALYSES ON THE SEISMIC RETROFITTING WITH ISOLATION FOR AN RC FRAME STRUCTURAL OFFICE BUILDING

Chenglin FAN[1], Junwu DAI[2], Yongqiang YANG[3]

ABSTRACT

The case office building located in Jingdezhen city of China, was built in 2005, which has been in use as an ordinary purpose of office building in the past 12 years. It is a four-story, single-span reinforced concrete frame structure. As the seismic design was not in consideration when it was designed and built, the seismic capacity of this structure is relatively lower than it should be as its new purpose of the local Earthquake Monitoring and Emergency Management Center. Because of its important role in future earthquake relief, the building's seismic fortification intensity is required to increase to 8 degrees (PGA=0.2g). According to the preliminary design analyses for all structural components of the original structure of the existing office building, both the axial compression ratio of columns and the reinforcement ratio of most beams and columns are not fit for the new seismic design requirement.

In this paper, finite element analyses for the base isolation system retrofitted with both of rubber bearings and lead rubber bearings are carried out for the updated structure of the existing office building. Also, the seismic analytical results comparison between the base isolated new structure and the original structure are carried out. Analyses results shows that both the cross-section enlargement strengthening for part of columns and steel wrapping strengthening for part of columns and beams are jointly used to withstand the earthquake requirements of 8 degrees (PGA=0.2g) design. Nonlinear analyses are conducted by using the ETABS program and the PKPM design software comparatively. Three possible isolation bearing arrangement schemes, including base isolation, the first-story-column-bottom isolation and the first-story-column-top isolation, are carried out and compared with each other. Finally, the first story column bottom isolation together with part of the beams and columns being strengthened is adopted as the retrofitting scheme for the office building.

Keywords: Seismic retrofitting; RC frame structure; Seismic isolation; Rubber bearing element strengthen

1. INTRODUCTION

Due to long-term use and structure change, the possible original structure bearing capacity may not meet the capacity requirements stipulated in the codes. In recent years, the maintenance and reinforcement of existing structure reinforcement technique has caused extensive concern of the engineering [1]. Isolation technology has significant advantages in vibration control and disaster reduction, as well as in social and economic benefits. The recent decades have witnessed a successful application of this technology in the field of architectural structures at home and abroad [2]. Enlarging section and wrapping section steel method are of strong adaptability, wide range of application, good reinforcement effect and durable performance. Meanwhile, these methods have mature design and construction experience and have been getting the attention of the engineering [3].

[1]Mr Chenglin Fan, Key Laboratory of Earthquake Engineering and Engineering Vibration, Institute of Engineering Mechanics, China Earthquake Administration, Harbin, China, 1171142524@qq.com

[2]Professor Junwu DAI, Structure Engineering, Key Laboratory of Earthquake Engineering and Engineering Vibration, Institute of Engineering Mechanics, China Earthquake Administration, Harbin, China, jwdai@iem.cn

[3]Associate Professor Yongqiang YANG, Structure Engineering, Key Laboratory of Earthquake Engineering and Engineering Vibration, Institute of Engineering Mechanics, China Earthquake Administration, Harbin, China, yangiem@foxmail.com

Based on the engineering example, the seismic isolation reinforcement of this structure was analyzed. Effects of different vibration isolation schemes were compared and analyzed respectively.

1.1 Basic information of the project site

The work status of the office building is shown in figures 1 and 2. According to "Code for seismic design of buildings" (GB50011-2010 in China), the site category is class Ⅱ, and the feature period is 0.35s. The basic seismic acceleration is 0.10g, the basic wind pressure is 0.40 kN/m^2, the basic snow pressure is 0.35 kN/m^2, and the shape factor of wind load is 1.3.

Figure 1. Front elevation

Figure 2. Back elevation

1.2 Storey size information

Detailed storey size data is listed in table 1.

Table 1. Equivalent dimensions of each layer (unit: m, m^2)

Storey number	Storey height	Area	Centroid(X,Y)	Equivalent wide	Equivalent height
5	2.4	16.52	10.90,2.95	2.80	5.90
4	3.1	189.42	11.55,4.10	23.10	8.20
3	3.1	189.42	11.55,4.10	23.10	8.20
2	3.1	189.42	11.55,4.10	23.10	8.20
1	3.3	189.42	11.55,4.10	23.10	8.20

1.3 Structural mass distribution

Detailed mass distribution data is listed in table 2.

Table 2. Mass distribution (unit: 10^3kg)

Storey number	Dead load quality	Live load quality	Layer quality	Mass ratio
5	15.5	1.2	16.8	0.09
4	178.7	14.8	193.5	0.71
3	251.3	20.2	271.5	1.00
2	251.2	20.2	271.3	1.03
1	242.9	20.2	263.0	1.00

Total dead load is 939.568×10^3 kg and the total live load is 76.545×10^3 kg. The total structure mass is 1016.112×10^3 kg. The mass distribution diagram and mass ratio diagram are shown in figures 3 and 4.

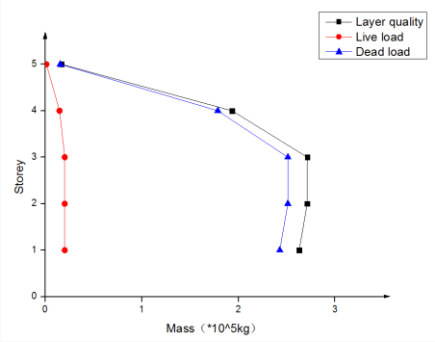

Figure 3. Mass distribution diagram

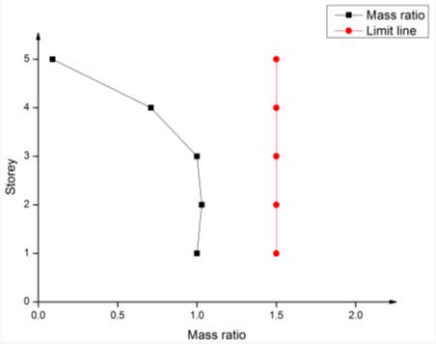

Figure 4. Mass ratio distribution diagram

1.4 Original construction profile

The structure contains seven frames, and there are three types of frameworks, KJ-1, KJ-2 and KJ-3 respectively. Structural standard layer design drawing is shown in figure 5. The frame column has three sections, KZ1(300*350 mm^2), KZ2(300*350 mm^2) and KZ3(350*400 mm^2) respectively. Sections of frame girder are 250*450 mm^2 and 250*500 mm^2. Secondary beam has two sections, they are 240*350 mm^2 and 300*500 mm^2. The cantilever beam has a variable section, the width is 250mm fixed, the height changes from 350 mm to 400 mm. The slab has a thickness of 100 mm and the thickness of the suspension plate is 70 mm. The beam, plate and column were cast in concrete C25, the stress tendon was HRB 335 and the stirrup was HPB 235.

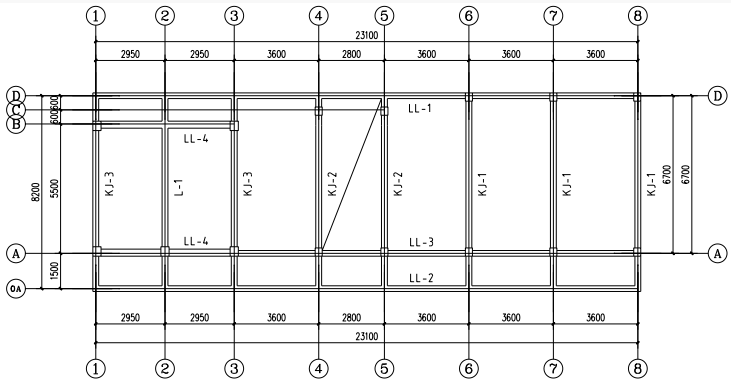

Figure 5. Structural standard layer design drawing

Under the condition of 8 degrees (PGA=0.2g), the axial compression ratio of columns exceeded the requirements and a serious shortage of beams and columns reinforcement was found. There were 12 columns in total of 14 columns in the first layer that had the phenomenon of the axial compression ratio of columns over-limited, and the maximum limit rate was up to 40%. On the second floor, there were two columns in jeopardy, but the state of the axial compression ratio of columns over-limited was not serious. There were 60 columns in the whole building from first to fifth floors, and there were three-fourths of the pillars that was 45 columns in a state of insufficient longitudinal reinforcement, including all columns on the first and second floors, 12 columns on the third floor and 5 columns on the fourth floor. There were 180 beams in the whole building, and nearly a third of the beams' longitudinal reinforcement and stirrups were not satisfied.

2. FEASIBILITY VERIFICATION

A modal analysis with ETABS program and the PKPM design software is conducted to obtain model quality and model period, which proves the high reliability of the used software. Detailed software models are shown in figures 6 and 7.

Figure 6. PKPM structure models

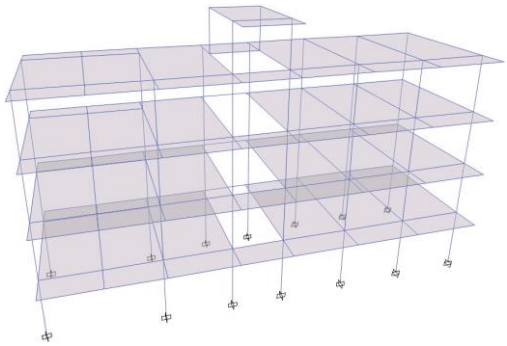

Figure 7. ETABS structure model

2.1 Comparison of model quality

Detailed comparison of model quality data is listed in table 3.

Table 3. Comparison of model quality (unit: ton)

PKPM non-isolation model	ETABS non-isolation model	Error (%)
1016.112	1016.142	0.003

By comparison, the conclusion shows that the difference between the model quality data of PKPM and ETABS is very small and meets the requirements.

2.2 Comparison of model period

Detailed comparison of model period data is listed in table 4.

Table 4. Comparison of model period (unit: s)

Mode of vibration	PKPM non-isolation model	ETABS non-isolation model
1	0.994	0.993
2	0.915	0.915
3	0.834	0.833
4	0.329	0.329
5	0.299	0.299
6	0.273	0.273
7	0.208	0.207
8	0.187	0.186
9	0.185	0.185
10	0.165	0.164
11	0.161	0.161
12	0.159	0.158
13	0.145	0.145
14	0.130	0.130
15	0.121	0.121

The sum of the PKPM modal participating mass ratio of the first 15 modes is 99.80%, which is larger than 90%. Meanwhile, the sum of the ETABS modal participating mass ratio of the first 15 modes is 99.80%, which is also enough. By comparison, the results show that there are hardly any differences between the model period data of PKPM and ETABS, and software reliability is high.

3. THE SELECTION OF GROUND MOTION RECORD

The case office building belongs to the key fortification buildings, which needs to be checked by using the time-history analysis method. According to "Code for seismic design of buildings" (GB50011-2010 in China), this project selects two actual ground motion records and one artificial simulated acceleration time-history curve, they are TH032TG035_CHI-CHI TAIWAN-06 9-25-1999 TCU075 (hereinafter referred to as TH032), TH036TG035_CHUETSU-OKI 7-16-2007 KAWAGUCHI (hereinafter referred to as TH036) and RH4TG035 (hereinafter referred to as RH4TG) respectively. All the acceleration time-histories are normalized. In the analysis process, the peak acceleration ratios of the three directions are set as X:Y:Z=1:0.85:0.65. Time-history curves of the earthquakes are shown in figure 8.

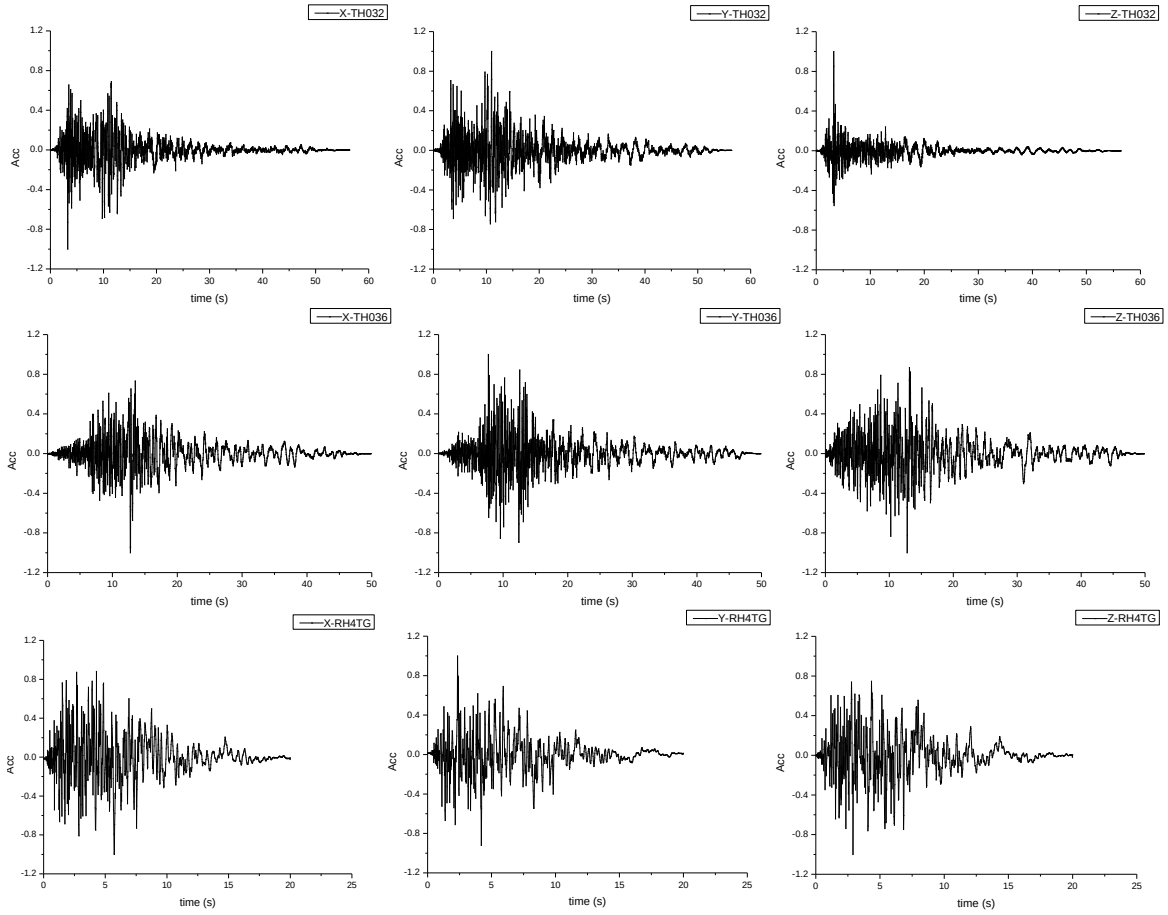

Figure 8. Time-history curves of TH032, TH036 and RH4TG

Comparison of ground motion acceleration spectra and target spectrum is shown in figure 9. According to "Code for seismic design of buildings", specification mandates that multiple sets of time-history of earthquake influence coefficient curve and vibration mode decomposition response spectrum method, compared to the seismic effect coefficient curve in corresponding to structure the main vibration mode cycle point of difference is not greater than 20%. Figure 9 shows that at the main period point of the first three modes of the structure, the difference between the influence coefficient of the mean time-history and the influence coefficient of the standard earthquake meets the specification requirements, they were 10.11%, 14.10%, 15.15%, respectively.

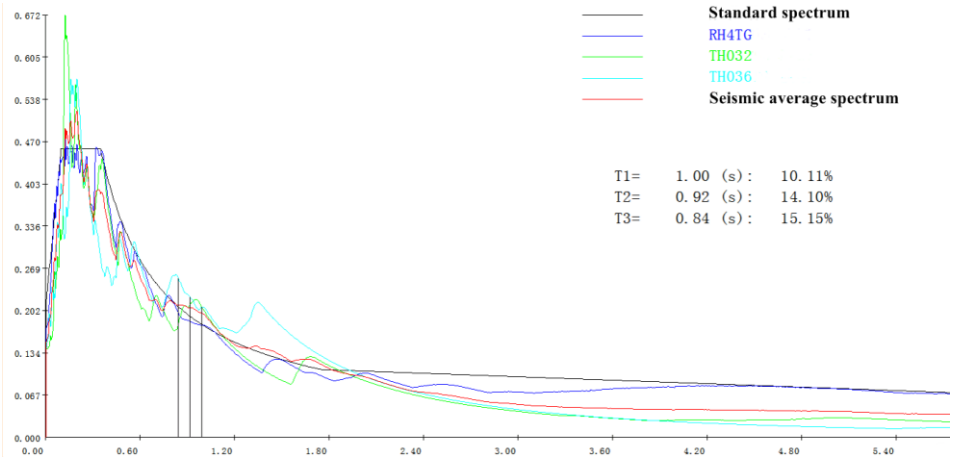

Figure 9. Comparison of ground motion acceleration spectrum and canonical spectrum

Using PKPM software, basis-shear forces of non-isolation structure are calculated. The comparison results are shown in table 5. The ratio is obtained by dividing basis-shear of each time-history by basis-shear of mode-superposition response spectrum method in the case of frequent earthquake.

Table 5. Basis-shear forces of non-isolation structure (unit: kN)

Working condition	Response spectrum	RH4TG	TH032	TH036	Average
X-shear	633.20	527.07	665.27	657.80	616.71
Y-shear	667.92	576.76	725.22	664.64	655.54
X-Ratio(%)	100	83.24	105.06	103.89	97.40
Y-Ratio(%)	100	86.35	108.58	99.51	98.15

4. LAYOUT OF ISOLATION LAYER

As a sudden natural disaster, the earthquake has plagued mankind, and the main way to mitigate the loss of life and property caused by the earthquake is the earthquake engineering. With the sound development of China's social and economic system, the traditional seismic design methods cannot meet the actual needs of the project, therefore, isolation design is becoming more and more popular.
There are three possible isolation bearing arrangement schemes for this consolidation project, including base isolation, the first-story-column-bottom isolation and the first-story-column-top isolation.
Three scenarios are described in detail below. The optimal scheme is selected by comparing the damping effect and feasibility in engineering practice. Finally, the first-story-column-bottom isolation scheme is chosen. The first-story-column-bottom isolation's results are explained in detail below, the other two methods are briefly described.

4.1 Selection of isolation bearings

4.1.1 Selection of isolation bearings

The performance parameters of the isolation bearings and the number of bearings used in this project are shown in tables 6 and 7 and the layout is shown in figure 10.

Table 6. Mechanical property parameters of natural rubber vibration isolation bearings (unit: set, kN/mm, mm)

Class	Quantity	Vertical stiffness	Horizontal stiffness	Preyield stiffness	Post-yield stiffness	Overall height of support
LNR400	6	1684.5	0.79	7.85	0.79	158

Table 7. Mechanical properties of lead-core rubber vibration isolation bearings (unit: set, kN/mm, kN, mm)

Class	Quantity	Vertical stiffness	Horizontal stiffness	Preyield stiffness	Post-yield stiffness	Yield force	Overall height of support
LRB400	8	1684.5	1.09	5.74	0.57	33.2	158

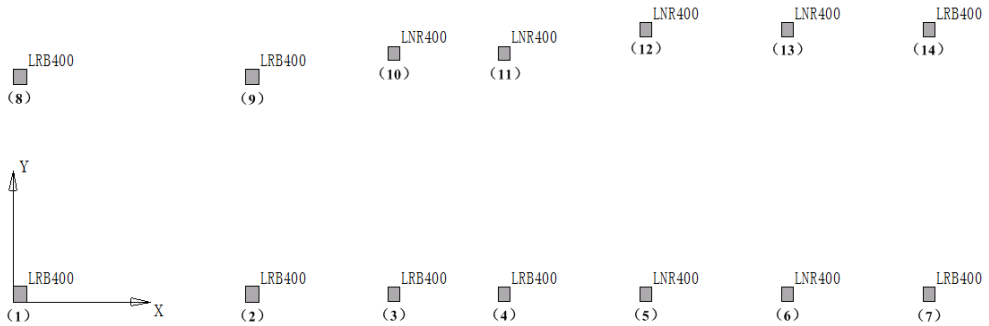

Figure 10. Detailed bearings layout

4.1.2 Malalignment checking calculation

The malalignment of the seismic isolation layer is an important index of the seismic isolation structure, Japanese and Taiwan norms clearly stipulates that the eccentricity should not exceed 3%. The eccentricity of the isolation layer is calculated as follows.
Barycentric coordinates are calculated by formula (1).

$$X_g = \frac{\sum N_{l,i} \cdot X_i}{\sum N_{l,i}}, Y_g = \frac{\sum N_{l,i} \cdot Y_i}{\sum N_{l,i}} \tag{1}$$

Center of stiffness coordinates are calculated by formula (2).

$$X_k = \frac{\sum K_{ey,i} \cdot X_i}{\sum K_{ey,i}}, Y_k = \frac{\sum K_{ex,i} \cdot Y_i}{\sum K_{ex,i}} \tag{2}$$

Offset is calculated by formula (3).

$$e_x = \left| Y_g - Y_k \right|, e_y = \left| X_g - X_k \right| \tag{3}$$

Torsional stiffness is calculated by formula (4).

$$K_t = \sum \left[K_{ex,i} \left(Y_i - Y_k \right)^2 + K_{ey,i} \left(X_i - X_k \right)^2 \right] \tag{4}$$

Elastic radius is calculated by formula (5).

$$R_x = \sqrt{\frac{K_t}{\sum K_{ex,i}}}, R_y = \sqrt{\frac{K_t}{\sum K_{ey,i}}} \tag{5}$$

The malalignment is calculated by formula (6).

$$\rho_x = \frac{e_y}{R_x}, \rho_y = \frac{e_x}{R_y} \tag{6}$$

In the equation, $N_{l,i}$ is the long-term axial load supported by the isolation bearing whose number is i; X_i and Y_i are the isolation bearing's X and Y direction center coordinates respectively, and the bearing's number is i; when the displacement delta appeared at the isolation layer, equivalent stiffness is obtained, and $K_{ex,i}$ and $K_{ey,i}$ are the number i isolation bearing's X and Y direction equivalent stiffness respectively. Detailed malalignment of the isolation layer data is listed in table 8. The position of the coordinate origin is shown in figure 10.

Table 8. Malalignment of the seismic isolation layer (unit: m, kN·m)

Coordinates	Barycentric	Center of stiffness	Offset	Torsional stiffness	Elastic radius	Malalignment (%)
X direction	11.28	11.28	0.05	1318959	8.17	0
Y direction	4.26	4.21	0.00			0.61

Calculated results show that the malalignment of the isolation layers at X and Y direction are 0% and 0.61% respectively, which is less than 3% and meet the requirements.

4.1.3 Compressive stress checking

The earthquake damage might cause casualties, direct and indirect economic losses, the case building's social influence degree and its role in earthquake relief are in consideration, according to the categories a fortified building for checking isolation bearing compressive stress. For first class buildings, the stress limit is 10 MPa. Under the influence of gravity load, the compressive stress of each bearing is given in table 9.

Table 9. Compressive stress of each bearing (unit: MPa)

Bearing number	Bearing type	Compressive stress
1	LRB400	5.81
2	LRB400	8.26
3	LRB400	6.15
4	LRB400	6.28
5	LNR400	6.43
6	LNR400	5.62
7	LRB400	4.51
8	LRB400	5.48
9	LRB400	7.49
10	LNR400	5.15
11	LNR400	5.00
12	LNR400	4.66
13	LNR400	3.85
14	LRB400	3.03

4.1.4 Anti - wind calculation of isolation layer

According to "Code for seismic design of buildings" (GB50011-2010 in China), the total horizontal force generated under wind load is unfavorable to 10% of total gravity of the structure. And the total yield of the isolation layer should be greater than 1.4 times the wind load of the structure.

For the case office building, the total horizontal force generated by the wind load of this structure is 151.7 kN, and the total gravity is 9957.90 kN, results meet the 10% requirement. The total yield force of the isolation layer is 33.2*8=265.6 kN > 1.4*151.7=212.38 kN, which meets the specification requirements.

4.2 Simulation of isolation bearings

A bilinear model is adopted for the horizontal constitutive relation of lead-core rubber vibration isolation bearings, as shown in figure 11. A linear elastic model is used for the horizontal constitutive relation of natural rubber vibration isolation. For the vertical constitutive relation of rubber isolation support, the tensile and compressive constitutive relations of the isolation support are linear elastic model, but the tensile stiffness is only 10% of the compressive stiffness.

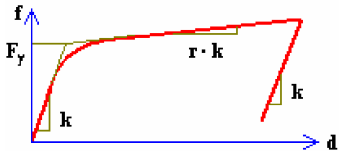

Figure 11. Horizontal constitutive relation

4.3 Base isolation scheme

This scheme sets 1.0 m high seismic isolation layer between the first layer of the bottom of the column and the top of the pile foundation, including the upper position of the 0.5 m is the foundation beam. Isolation bearing is 158 mm high, it locates below the foundation beam and is 200 mm apart from the bottom surface. To increase security, the top of the pile foundation needs to be reinforced about 300 mm.

4.4 The first-story-column-bottom isolation scheme

In this scheme, the height of 158 mm (the upper and lower plates are 20 mm thick) isolation bearings are located at the height of 500 mm above the bottom of the columns. It is needed to reinforce the 500 mm column piers below the isolation bearings. The joists of 240*350 mm^2 are added to the upper of the bearings and closes to them. The joists layout is shown in figure 12.

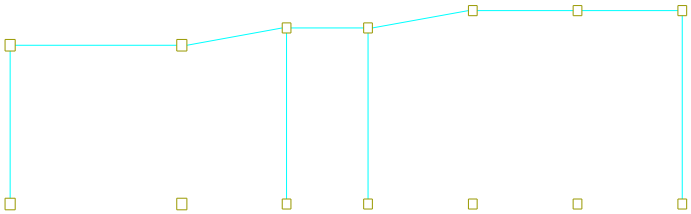

Figure 12. The joists layout

4.5 The first-story-column-top isolation scheme

In this method, the height of 158 mm isolation bearings are located at the top of first story columns, the joists of 240*350 mm^2 are added under the bearings and closes to them.

4.6 Comparison and selection of three isolation bearing arrangement schemes

Overturning moment reduction ratio, which is only needed for high-rise buildings, is not needed for the multistorey buildings, which is researched in this paper. Three sets of tri-dimensional ground motions, scaled at PGA 0.2g, are used and ETABS is chosen to conduct the finite element analyses. Dynamic responses of the building with and without isolation are compared. Detailed comparison of shear force

reduction ratio data is listed in table 10.

Table 10. Shear force reduction ratio

Base isolation	The first-story-column-bottom isolation	The first-story-column-top isolation
0.670	0.399	0.400

Combined with the actual situation of the project, the degree of difficulty of construction and the amount of reinforcement after using isolation technology, the first-story-column-bottom isolation scheme requires the least reinforcement, easy construction and little influence on structure. Finally, the first-story-column-bottom isolation scheme is chosen.

4.7 The maximum influence impact coefficient of the structure above the isolation layer

According to "Code for seismic design of buildings" (GB50011-2010 in China), the maximum seismic impact coefficient can be calculated according to the following formula (7).

$$\alpha_{max1} = \beta\alpha_{max} / \psi \tag{7}$$

In the equation, α_{max1} is the maximum horizontal seismic impact coefficient of isolation structure; α_{max} is the maximum horizontal seismic influence coefficient of non-isolation structure is adopted in accordance with section 5.1.4 of this regulation; β is the shear force reduction ratio; ψ is the adjustment coefficient, for general rubber vibration isolation bearing is 0.8.
Finally, the maximum seismic influence coefficient of the structure above the seismic isolation layer is calculated according to equation (8).

$$\alpha_{max1} = \beta\alpha_{max} / \psi = 0.399 \times 0.16 / 0.8 \approx 0.08 \tag{8}$$

4.7 The relevant modal shapes of the building, non-isolated and isolated

Detailed modal shape of the non-isolated building and isolated building are listed in figures 13 and 14.

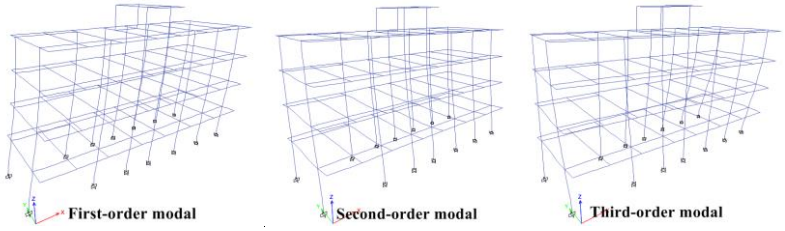

Figure 13. The modal shape of the non-isolated building modeling

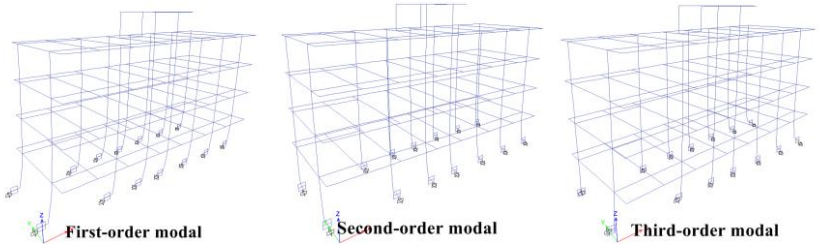

Figure 14. The modal shape of the isolated building modeling

5. CONCLUSIONS

The first three periods of the seismic isolation structure are 1.895 s, 1.825 s and 1.663s, the first two steps are the translational period, the third order is the torsional period, and the vibration isolation greatly extends the structure self-oscillation period, which reduces the structural response of the earthquake. The structure periods have been greatly extended. The shear force reduction ratio of the seismic isolation structure is 0.399, less than 0.40, which is required by the seismic code, and the seismic measures of the isolation layer above structures are reduced by 1 degree. The structure above the seismic isolation layer would be calculated by 7 degrees (PGA=0.1g), and the construction measures are calculated according to the secondary framework, and the axial compression ratio of the frame column is 0.75.

The isolation method solves the problem of the axial compression ratio and the insufficient reinforcement of a considerable part of the structure. The final reinforcement method and the optimum location of reinforcement placement are determined. The reinforcement method of enlarging section and wrapping section steel are adopted in the reinforcement of this project. The structure reinforcement planes are shown in figures 15 to 19.

In addition, checking of the maximum displacement of the isolation bearings is carried out. The maximum horizontal displacement of the isolation bearings is 112.27 mm, smaller than 0.55D (D is the diameter of bearings, which is 220mm) and 3Tr (Tr is the total rubber layer thickness, which is 192 mm), which meets the requirements. Besides, the calculation of bearings' maximum stress and the interlayer displacement angle of reinforced structure satisfies the requirements.

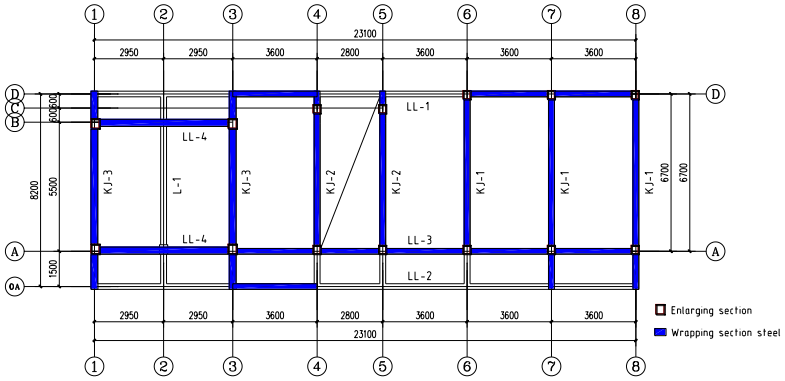

Figure 15. The first layer structure reinforcement plane

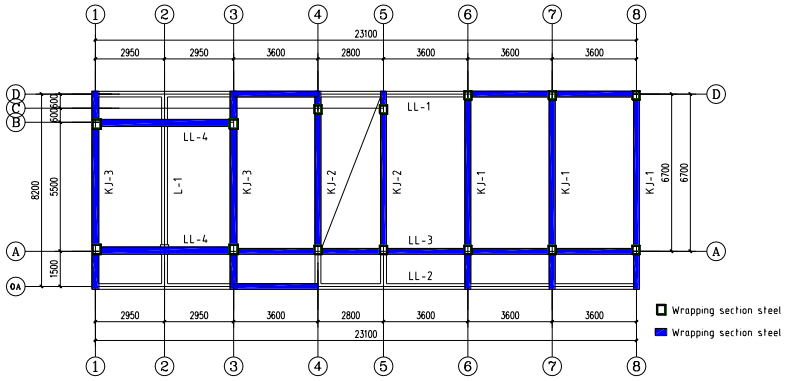

Figure 16. The second layer structure reinforcement plane

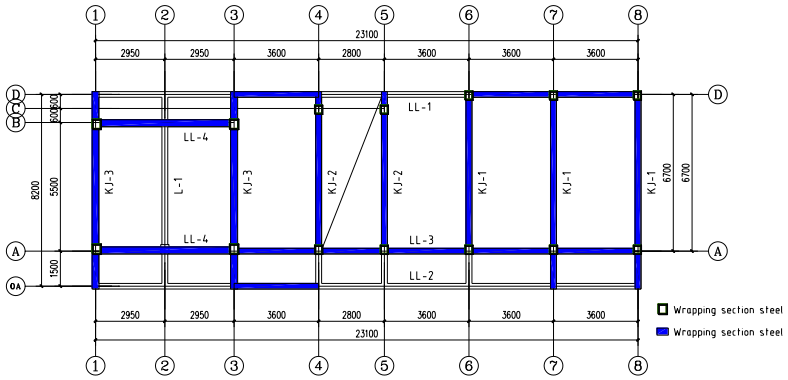

Figure 17. The third layer structure reinforcement plane

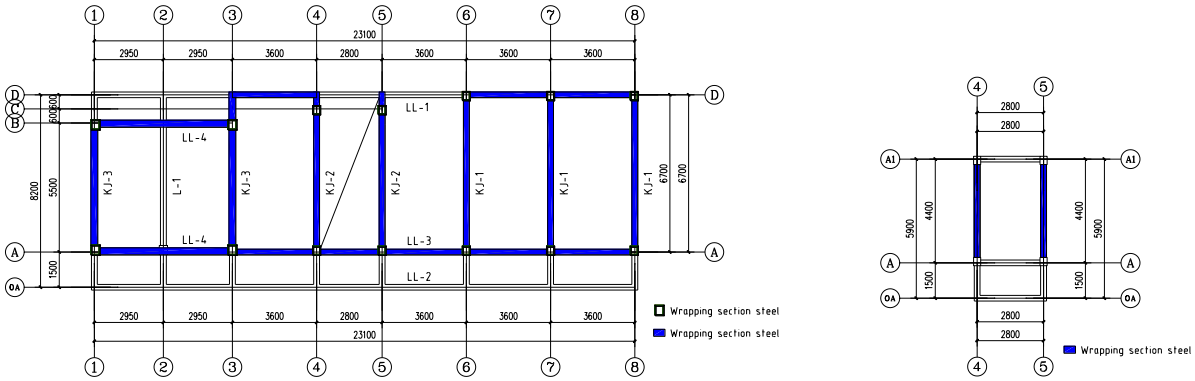

(a) The fourth layer (b) The fifth layer

Figure 18. and Figure 19. The fourth layer and the fifth layer structure reinforcement plane

6. ACKNOWLEDGMENTS

The authors gratefully acknowledge the financial support provided by the Scientific Research Fund of IEM, CEA (2017A01), the Urban Engineering System Earthquake Safety and Recovery Evaluation Theory Research Program (201508023) and Program for Innovative Research Team in China Earthquake Administration.

7. REFERENCES

Yixuan L (2015). Study on seismic behavior of RC frame strengthened by enlarging section method. *Construction technology*, 46(08): 73-732. (in Chinese)

Hongping Z, Fangyuan Z, Yong Y (2014). Development and analysis of the research on base isolation structures. *Engineering mechanics*, 31(03):1-10. (in Chinese)

Jianfeng H, Chunming Z, Zhiguo G (2013). Experimental study on seismic behavior of earthquake-damaged RC frame strengthened by enlarging cross-section. *Journal of civil engineering*, 45(12): 9-17. (in Chinese)